**Noname manuscript No.**
(will be inserted by the editor)

# Composite observer-based adaptive dynamic surface control for fractional-order nonlinear systems with input saturation

**Zhiye Bai**[1] · **Shenggang Li**[2] · **Heng Liu**[3,*]

Received: date / Accepted: date

**Abstract** This article proposes an adaptive neural output feedback control scheme in combination with state and disturbance observers for uncertain fractional-order nonlinear systems containing unknown external disturbance, input saturation and immeasurable state. The radial basis function neural network (RBFNN) approximation is used to estimate unknown nonlinear function, and a state observer as well as a fractional-order disturbance observer is developed simultaneously by using the approximation output of the RBFNN to estimate immeasurable states and unknown compounded disturbances, respectively. Then, a fractional-order auxiliary system is constructed to compensate the effects caused by the saturated input. In addition, by introducing a dynamic surface control strategy, the tedious analytic computation of time derivatives of virtual control laws in the conventional backstepping method is avoided. The proposed method guarantees that the boundness of all signals in the closed loop system and the tracking errors converge to a small neighbourhood around the origin. Finally, two examples are provided to verify the effectiveness of the proposed control method.

**Keywords** State observer · disturbance observer · neural network · fractional-order nonlinear system · dynamic surface control

## 1 Introduction

Although fractional calculus was mentioned more than three hundred years, its research has been focused on the field of mathematical sciences because of

* Corresponding author.E-mail: liuheng122@gmail.com
[1]College of Mathematics and Information Science, Shaanxi Normal University, Xi'an 710119, China
[2]College of Mathematics and Information Science, Shaanxi Normal University, Xi'an 710119, China
[3]School of Science, Guangxi University for Nationalities, Nanning 530006, China

the lack of actual physical meaning. Until recent decades, the applications of fractional calculus have developed rapidly and received enormous attention due to the fact that fractional calculus can model a real object more precisely than the traditional integer-order method in the fields of system control, heat conduction electronic, signal processing and secure communication and so forth [1–4]. For this reason, the fractional-order nonlinear systems (FONSs) have received considerable attention from scholars, whose control design have become one of the research hotspots in the past few years. So far, a number of control methods have been derived for the FONSs by integrating some classic control approaches including sliding mode control, fuzzy or neural network control and adaptive control [5–8]. Nevertheless, the controller design for FONSs is still insufficient because some constraints are usually ignored, such as model uncertainty, saturated nonlinearity, and immeasurable state. In addition, it is worthwhile pointing out that control approaches of integer-order systems may not be directly extended to fractional-order systems because of the special characteristics of fractional calculus. Therefore, more robust tracking control schemes should be further exploited for FONSs aiming to solve the aforementioned limitations.

It is well known that the strict feedback system is a common type of nonlinear systems, and many physical models can be described as this structure, such as inverted pendulum, oscillator, single machine infinite bus power supply box and quarter-car active suspension model [9–12]. One of the most powerful methods for the stability analysis of this type of systems is the backstepping technique. In recent years, some scholars have investigated the backstepping control of FONSs, and some valuable results have also been reported. In [13], an efficient controller was designed for fractional-order chaotic systems by blending Mittag-Leffler function and Lyapunov stability results with backstepping technique, which not only ensures global stability of systems but also avoids the singularity problem. By combining with a fractional-order sliding mode surface and a disturbance observer, a command filter based backstepping control scheme was exploited for FONSs with disturbance in [14]. In the above literature, the priori knowledge of system models and matching condition are necessary. However, the accurate model of system nonlinearities is hard to be directly obtained in practice because system uncertainties such as uncertain parameters or functions, modeling errors and external disturbances are unavoidable. An effective method for uncertain FONSs with strict feedback is adaptive fuzzy or neural network control strategy based on backstepping technique because system uncertainties can be tackled by fuzzy logical systems (FLSs) or neural networks. For example, in the light of the backstepping approach, an adaptive neural control scheme for uncertain FONSs was presented in [15], where both full state constraints and input saturation are considered, and a barrier Lyapunov function is introduced to prevent the violation of full state constraints. In [16,17], an adaptive backsteeping tracking control scheme was developed successively for FONSs with unknown nonlinearities and external disturbances, where the system model is fully unknown. It should be pointed out that, in the above literature, to avoid the issue of explosion of com-

plexity, the FLSs or neural networks are employed to estimate the fractional derivatives of virtual controllers; however, this approach will bring accumulated fuzzy approximation errors, which will degrade the control performance of the system. A feasible method to solve this problem is using the dynamic surface control (DSC), whose main idea consists in that the derivative of virtual control inputs are substituted by some algebraic terms. In [18], both adaptive DSC and composite learning DSC were developed for uncertain FONSs, in which fractional derivative of intermediate control function can be calculated easily in each backstepping step by a fractional dynamic surface. Aiming at the filed of SISO strict feedback uncertain FONSs with external disturbances, by combining the FLSs and the DSC technique, a novel adaptive output feedback control method was designed in [19], where an auxiliary function is introduced to erase the possible chattering phenomenon. Although adaptive fuzzy or neural backstepping control combined with the DSC technique can solve the the issue of explosion of complexity, aforementioned control schemes are put forward based on the assumption that the states of controlled systems can be obtained directly.

However, in real-world systems, it is difficult or even impossible to access directly the whole state variables due to fact that the application of sensors will require larger machine sizes and additional drive costs, thereby the only information one can get is the system output in most instances. To cope with this limitation, an effective method is to develop a state observer in advance to estimate unknown states. Over the last few years, some observer-based adaptive control schemes were proposed for FONSs. Ref. [20] focused on the observer-based tracking control of incommensurate fractional-order systems, and a novel sliding surface combined with output feedback control strategy, which is qualified for not only state estimation but also tracking, was proposed. For incommensurate fractional-order systems with immeasurable states and uncertain parameters, an observer-based adaptive backstepping controller was developed in [21], where the input saturation is taken into account, and a fractional-order auxiliary system is designed to compensate for the saturation. In [22], for a fractional-order chaotic permanent magnet synchronous motor with the immeasurable states and unknown nonlinear functions, to reduce hardware complexity and costs, an adaptive neural network reduced order state observer in combination with the backstepping technique was proposed. By appropriately selecting gain matrix, the state observer could estimate the immeasurable states well and estimation errors converged to a small neighborhood of the origin in [23], where a super twisting algorithm is employed to avoid repeatedly differentiating the intermediate control function in the framework of backstepping. Although the aforementioned work effectively solved the problem of unknown states by a state observer, the system models constraints are relatively strict, and the system models are relatively simple without considering external disturbances which usually degrade the performance of system, or even result in instability. To strengthen the robustness of the system, the method of compensating the maximum disturbance boundary was adopted for FONSs in [16, 19, 24, 25]; however, very large controller gains should be

used to guarantee the convergence of the tracking error. Thus, it is important to investigate the method of disturbance estimate, which can improve the control accuracy and reduce the energy consumption. However, to the best of the author's knowledge, the state observer and disturbance observer are rarely considered simultaneously due to fact that it is very hard to tackle the two observation errors. Consequentially, how to solve this problem is a meaning but challenging work.

Motivated by the above discusses, the main purpose of this paper is to develop a observer-based adaptive backstepping DSC technology for FONSs in the presence of unmeasured state, input saturation and external disturbance. Compared with the existing results, the main contributions of this paper can be summarized as follows. (1) Different from [20–23, 26–29], which only consider a state observer or a disturbance observer, two observers are designed at the same time in this paper. (2) An observer-based fractional-order DSC strategy is designed for FONSs with input saturation and external disturbance.

The rest of this paper is structured as follows. Some preliminaries and the problem formulation are given in Section 2. In Section 3, a state observer and a disturbance observer are constructed simultaneously firstly, and then a controller is designed based on the adaptive neural backstepping control method. In Section 4, two simulation examples are given to illustrate the effectiveness of the proposed method. Finally, some conclusions are given in Section 5.

## 2 Preliminaries and Problem description

### 2.1 Preliminaries

In this part, some basic definitions of fractional calculus and useful lemmas are introduced. The Caputo definition, which can be used in engineering applications widely because its initial value condition has important physical meaning, is employed.

**Definition 1** [30] The Caputo fractional integral of a smooth function $f(t)$ with respect to $t$ and the lower terminal 0 is expressed as

$$ {}_0^C\mathcal{D}_t^{-\nu} f(t) = \frac{1}{\Gamma(\nu)} \int_0^t \frac{f(\tau)}{(t-\tau)^{1-\nu}} d\tau, \tag{1} $$

where $\Gamma(\cdot)$ represents the Gamma function.

**Definition 2** [30] The Caputo fractional derivative of a continuous function $f(t)$ can be defined as

$$ {}_0^C\mathcal{D}_t^{\nu} f(t) = \frac{1}{\Gamma(\omega-\nu)} \int_0^t \frac{f^{(\omega)}(\tau)}{(t-\tau)^{\nu+1-\omega}} d\tau, \tag{2} $$

where $\omega - 1 < \nu < \omega$ and $\omega \in \mathbb{N}^+$.

The Laplace transform of (2) is given by

$$\mathscr{L}({}_0^C\mathcal{D}_t^\nu f(t); s) = s^\nu F(s) - \sum_{k_0=0}^{n-1} s^{\nu-k_0-1} f^{(k_0)}(0), \tag{3}$$

where $F(s) = \mathscr{L}(f(t)) = \int_0^\infty e^{-st} f(t)dt$. For convenience, in the following part of this paper, only the case that $\nu \in (0, 1)$ is considered, and $\mathcal{D}^\nu$ is used to replace ${}_0^C\mathcal{D}_t^\nu$.

**Definition 3** [30] The Mittag-Leffler function with two parameters is represented as

$$E_{\nu_1,\nu_2}(x) = \sum_{j=1}^{\infty} \frac{x^j}{\Gamma(\nu_1 j + \nu_2)}, \tag{4}$$

where $\nu_1, \nu_2 > 0$, and $x$ is a complex number. Furthermore, take the Laplace transform on (4), one has

$$\mathscr{L}\{t^{\nu_2-1} E_{\nu_1,\nu_2}(-\zeta t^{\nu_1})\} = \frac{s^{\nu_1-\nu_2}}{s^{\nu_1} + \zeta}, \tag{5}$$

in which $\zeta \in \mathbb{R}$.

**Lemma 1** *[31] Let $x(t) \in \mathbb{R}$ be a continuous and differentiable function. Then, for any time instant $t > t_0$, the following inequality holds*

$$\mathcal{D}^\nu x^2(t) \leq 2x(t)\mathcal{D}^\nu x(t). \tag{6}$$

Moreover, suppose that $\mathbf{x}(t) \in \mathbb{R}^n$, it holds

$$\mathcal{D}^\nu(\mathbf{x}^T(t)\mathbf{P}\mathbf{x}(t)) \leq 2\mathbf{x}^T(t)\mathbf{P}\mathcal{D}^\nu\mathbf{x}(t), \tag{7}$$

where $\mathbf{P} = \mathbf{P}^T \in \mathbb{R}^{n\times n}$ is a positive definite matrix.

**Lemma 2** *[16] For a complex number $\nu_2$ and two real numbers $\nu_1$, $\bar{\nu}$ satisfying $0 < \nu_1 < 2$ and $\frac{\nu_1\pi}{2} < \bar{\nu} < \min\{\pi, \pi\nu_1\}$, the following equation holds*

$$E_{\nu_1,\nu_2}(\zeta) = -\sum_{j=1}^{m} \frac{1}{\Gamma(\nu_2 - \nu_1 j)\zeta^j} + o(|\zeta|^{-1-m}), |\zeta| \to \infty, \bar{\nu} \leq |arg(\zeta)| \leq \pi, \tag{8}$$

*for all integer $m \geq 1$.*

**Lemma 3** *[16] Let $\nu_1 \in (0, 2)$ and $\nu_2$ be an arbitrary real number. If a real number $\bar{\nu}$ satisfies $\frac{\nu_1\pi}{2} < \bar{\nu} < \min\{\pi, \pi\nu_1\}$, the following equation exists*

$$|E_{\nu_1,\nu_2}(\zeta)| \leq \frac{\epsilon}{1 + |\zeta|}, \tag{9}$$

*where $\epsilon > 0$, $\bar{\nu} \leq |\arg(\zeta)| \leq \pi$, and $|\zeta| \geq 0$.*

**Lemma 4** *[32] Consider the following fractional-order system, if the $\nu$-th derivative of Lyapunov function $V(t)$ satisfies*

$$\mathcal{D}^{\nu}V(t) \leq -b_1V(t) + b_2, \tag{10}$$

*where $\nu \in (0,1)$, $b_1 > 0$ and $b_2 > 0$, then one has*

$$V(t) \leq V(0)E_{\nu}(-b_1t^{\nu}) + \frac{b_2\varrho}{b_1}, \tag{11}$$

*where $\varrho = \max\{1, \epsilon\}$ and $\epsilon$ is defined in Lemma 3.*

## 2.2 System Descriptions and Assumptions

Consider uncertain strict feedback FONSs with input saturation and time varying disturbances in the following form

$$\begin{cases} \mathcal{D}^{\nu}\xi_i = \xi_{i+1} + f_i(\bar{\boldsymbol{\xi}}_i) + d_i(t), 1 \leq i \leq n-1, \\ \mathcal{D}^{\nu}\xi_n = u(v) + f_n(\bar{\boldsymbol{\xi}}_n) + d_n(t), \\ y = \xi_1, \end{cases} \tag{12}$$

where $\bar{\boldsymbol{\xi}}_i = [\xi_1, \xi_2, \cdots, \xi_i]^T \in \mathbb{R}^i$ is the system state vector, and $y \in \mathbb{R}$ is the output of system; $f_i(\bar{\boldsymbol{\xi}}_i)$ is an unknown continuous nonlinear function, and $d_i(t)$ is an unknown external time varying disturbance; $v$ stands for system control input; and $u(v)$ is the input saturation function, which is described by

$$u(v) = sat(v) = \begin{cases} u_M, & v \geq u_M, \\ v, & u_m < v < u_M, \\ u_m, & v \leq u_m, \end{cases} \tag{13}$$

where $u_M > 0$ and $u_m < 0$ are known saturation amplitudes. According to (13), one obtains $u(v) = v + \Delta u$, where $\Delta u$ is the different between $v$ and $u(v)$.

Let $y_d$ be a reference signal, and assume that only the output signal $y$ is measurable. The purpose of this paper is to design an adaptive neural controller based on a state observer and a disturbance observer so that all the signals are bounded, and the output $y$ can follow the desired reference signal $y_d$ as closely as possible. To facilitate controller design, one needs the following assumptions.

**Assumption 1** *The referenced signal $x_d(t)$ and its $\vartheta$-th derivative $D_t^{\vartheta}x_d(t)$ are bounded and known.*

**Assumption 2** *For the external disturbance $d_i(t)$ in the system (12), there exist unknown positive constants $\bar{d}_{i1}$, $\bar{d}_{i2}$ such that $|d_i(t)| \leq \bar{d}_{i1}$ and $|\mathcal{D}^{\nu}d_i(t)| \leq \bar{d}_{i2}$.*

**Assumption 3** *There exists a known positive constant $L_i$ such that the following equality holds*

$$|f_i(\bar{\boldsymbol{\xi}}_i) - f_i(\hat{\bar{\boldsymbol{\xi}}}_i)| \leq L_i||\bar{\boldsymbol{\xi}}_i - \hat{\bar{\boldsymbol{\xi}}}_i||, \tag{14}$$

where $\hat{\bar{\boldsymbol{\xi}}}_i = [\hat{\xi}_1, \hat{\xi}_2, \cdots, \hat{\xi}_i]^T$ is the estimation of $\bar{\boldsymbol{\xi}}_i = [\xi_1, \xi_2, \cdots, \xi_i]^T$, and $||*||$ denotes the Euclidean norm.

### 2.3 RBFNN

In this paper, the RBFNN is employed to estimate the unknown nonlinear smooth function $f(X) : \mathbb{R}^\ell \to \mathbb{R}$, which can be expressed by

$$f(X) = \boldsymbol{\theta}^T \boldsymbol{\vartheta}(X),$$

where $\boldsymbol{\theta} = [\theta_1, \theta_2, \cdots, \theta_p]^T \in \mathbb{R}^p$ is the weight vector and $p > 1$ is the number of the neural network. $X \in \mathbb{R}^p$ is the input vector and $\ell$ is the input dimension. $\boldsymbol{\vartheta}(X) = [\vartheta_1(X), \vartheta_2(X), \cdots, \vartheta_p(X)]^T$ means the basis function vector, which is chosen as

$$\vartheta_\jmath(X) = \exp\Big[-\frac{(X - \mathbf{c}_\jmath)^T(X - \mathbf{c}_\jmath)}{\varsigma_\jmath^2}\Big], \jmath = 1, 2, \cdots, p,$$

where $\mathbf{c}_\jmath = [c_{\jmath 1}, c_{\jmath 2}, \cdots, c_{\jmath q}]^T$ is the center of the receptive and $\varsigma_\jmath$ is the width of the basis function $\vartheta_\jmath(X)$. From the definition of $\boldsymbol{\vartheta}(X)$ in [33,34], one obtains that $\boldsymbol{\vartheta}(X)$ is bounded with upper bound $a$ $(0 \leq a \leq 1)$, i.e.,

$$||\boldsymbol{\vartheta}(X)|| \leq a. \tag{15}$$

Based on the above discussion, the neural network can estimate $f(X)$ to an arbitrary accuracy in the compact set $\Omega_X \in \mathbb{R}^q$ by selecting sufficiently large node number $p$ as

$$f(X) = \boldsymbol{\theta}^{*T} \boldsymbol{\vartheta}(X) + \varepsilon(X), \tag{16}$$

where $\boldsymbol{\theta}^*$ is the ideal weight vector and defined as

$$\theta^* = \arg\min_{\hat{\theta} \in \mathbb{R}^p} \Big\{ \sup_{X \in \Omega_X} |f(X) - \boldsymbol{\theta}^T \boldsymbol{\vartheta}(X)| \Big\}$$

and $\varepsilon(X)$ denotes the approximation error and satisfies $\varepsilon(X) \leq \bar{\varepsilon}(\bar{\varepsilon} \geq 0)$.

*Remark 1* Because the immeasurable state $\xi_i$, the unknown smooth function $f_i(\cdot)$, the external disturbance $d_i(t)$ and the control input saturation $u(v)$ exist at the same time, the controller design for the FONS (12) becomes very complicated. The time dependent disturbance $d_i(t)$ relies heavily on exogenous effect, so one can conclude that the disturbance and the time derivative of the disturbance are bounded, that is, Assumption 2 is reasonable. On the other hand, the difference $\Delta u$ between the actual control input $v(t)$ and the saturation input $u(v)$ is bounded because only the finite control moment or control force can be provided for practical systems in industry.

According to the above discussion, the system (12) can be described as

$$\begin{cases} \mathcal{D}^{\nu}\xi_i = \xi_{i+1} + f_i(\hat{\bar{\boldsymbol{\xi}}}_i) + \Delta f_i + d_i(t), 1 \le i \le n-1, \\ \mathcal{D}^{\nu}\xi_n = u(v) + f_n(\hat{\bar{\boldsymbol{\xi}}}_n) + \Delta f_n + d_n(t), \\ y = \xi_1, \end{cases} \tag{17}$$

where $\Delta f_i = f_i(\bar{\boldsymbol{\xi}}_i) - f_i(\hat{\bar{\boldsymbol{\xi}}}_i)$.

Since $f_i(\hat{\bar{\boldsymbol{\xi}}}_i)$ is unknown, it can be approximated as

$$r_i f_i(\hat{\bar{\boldsymbol{\xi}}}_i) = \boldsymbol{\theta}_i^{*T}\boldsymbol{\vartheta}_i(\hat{\bar{\boldsymbol{\xi}}}_i) + \varepsilon_i(\hat{\bar{\boldsymbol{\xi}}}_i), \tag{18}$$

where $\boldsymbol{\theta}_i^*$ is the optimal weight vector, and $\varepsilon_i(\hat{\bar{\boldsymbol{\xi}}}_i)$ is the approximation error. By substituting (18) into (17), the uncertain nonlinear system (17) can be rewritten as

$$\begin{cases} \mathcal{D}^{\nu}\xi_i = \xi_{i+1} + \dfrac{1}{r_i}\boldsymbol{\theta}_i^{*T}\boldsymbol{\vartheta}_i(\hat{\bar{\boldsymbol{\xi}}}_i) + \delta_i, \\ \mathcal{D}^{\nu}\xi_n = u(v) + \dfrac{1}{r_n}\boldsymbol{\theta}_n^{*T}\boldsymbol{\vartheta}_n(\hat{\bar{\boldsymbol{\xi}}}_n) + \delta_n, \\ y = \xi_1, \end{cases} \tag{19}$$

where $\delta_i = \Delta f_i + \frac{1}{r_i}\varepsilon_i(\hat{\bar{\boldsymbol{\xi}}}_i) + d_i(t)$.

*Remark 2* The signal $\delta_i$ is called the unknown compound disturbance, which is composed of external time varying disturbance $d_i(t)$, neural optimal approximation error $\varepsilon_i(\hat{\bar{\boldsymbol{\xi}}}_i)$ and $\Delta f_i$. According to Assumptions 2, 3 and the approximation of ability of the neural network, the time derivative of the compound disturbance is bounded, i.e., $|\mathcal{D}^{\nu}\delta_i| \le \bar{\delta}_i$, where $\bar{\delta}_i$ is an unknown positive constant.

## 3 Main Results

In this section, a state observer and a disturbance observer are developed to estimate the unmeasurable states and the unknown compound disturbances, respectively. Then, a backstepping design procedure will be established for uncertain strict feedback FONSs under the adaptive neural control framework.

### 3.1 Composite observer design

To observe the unmeasurable system state $\xi_i$, a state observer is designed as

$$\begin{cases} \mathcal{D}^{\nu}\hat{\xi}_i = \hat{\xi}_{i+1} + \dfrac{1}{r_i}\hat{\boldsymbol{\theta}}_i^{T}\boldsymbol{\vartheta}_i(\hat{\bar{\boldsymbol{\xi}}}_i) + m_i(y - \hat{\xi}_1) + \hat{\delta}_i, \\ \mathcal{D}^{\nu}\hat{\xi}_n = u(v) + \dfrac{1}{r_n}\hat{\boldsymbol{\theta}}_n^{T}\boldsymbol{\vartheta}_n(\hat{\bar{\boldsymbol{\xi}}}_n) + m_n(y - \hat{\xi}_1) + \hat{\delta}_n, \\ \hat{y} = \hat{\xi}_1, \end{cases} \tag{20}$$

where $\hat{\boldsymbol{\theta}}_i$ is parameter weight vector which is employed to approximate ideal weight vector $\boldsymbol{\theta}_i^*$, and $\hat{\delta}_i$ is the estimation of the compounded disturbance $\delta_i$. Define the estimation errors $\tilde{\xi}_i = \xi_i - \hat{\xi}_i$, $\tilde{\boldsymbol{\theta}}_i = \boldsymbol{\theta}_i^* - \hat{\boldsymbol{\theta}}_i$, $\tilde{\delta}_i = \delta_i - \hat{\delta}_i$ and $\tilde{y} = y - \hat{y}$. From (19) and (20), one has

$$\begin{cases} \mathcal{D}^{\nu}\tilde{\boldsymbol{\xi}} = \mathbf{A}\tilde{\boldsymbol{\xi}} + \tilde{\boldsymbol{\Theta}} + \tilde{\boldsymbol{\delta}} \\ \tilde{y} = \mathbf{C}^T\tilde{\xi}_1, \end{cases} \tag{21}$$

where $\tilde{\boldsymbol{\xi}} = [\tilde{\xi}_1, \tilde{\xi}_2, \cdots, \tilde{\xi}_n]^T$, $\tilde{\boldsymbol{\Theta}} = \left[\frac{1}{r_1}\tilde{\boldsymbol{\theta}}_1^T\boldsymbol{\vartheta}_1(\hat{\tilde{\boldsymbol{\xi}}}_1), \frac{1}{r_2}\tilde{\boldsymbol{\theta}}_2^T\boldsymbol{\vartheta}_2(\hat{\tilde{\boldsymbol{\xi}}}_2), \cdots, \frac{1}{r_n}\tilde{\boldsymbol{\theta}}_n^T\boldsymbol{\vartheta}_n(\hat{\tilde{\boldsymbol{\xi}}}_n)\right]^T$, $\tilde{\boldsymbol{\delta}} = [\tilde{\delta}_1, \tilde{\delta}_2, \cdots, \tilde{\delta}_n]^T$, $\mathbf{C} = [1, 0, \cdots, 0]^T$, $\mathbf{A} = \begin{pmatrix} \mathbf{A}_1 & \mathbf{A}_2 \\ \mathbf{A}_3 & \mathbf{A}_4 \end{pmatrix}$, and $\mathbf{A}_1 = [-m_1, \cdots, -m_{n-1}]^T$, $\mathbf{A}_2 = I_{n-1\times n-1}$, $\mathbf{A}_3 = -m_n$, $\mathbf{A}_4 = [0, 0, \cdots, 0]_{n-1}$ and $m_i$ is the observation gain parameter to be decided. At the same time, the designed parameter $m_i$ is chosen so that the polynomial $p(s) = s^n + m_1 s^{n-1} + \cdots + m_{n-1}s + m_n$ is Hurwitz. Therefore, for a positive definite matrix $\mathbf{P} = \mathbf{P}^T \in \mathbb{R}^{n\times n}$, there exists a positive definite matrix $\mathbf{Q} = \mathbf{Q}^T \in \mathbb{R}^{n\times n}$ such that

$$\mathbf{A}^T\mathbf{P} + \mathbf{P}\mathbf{A} \leq -\mathbf{Q}. \tag{22}$$

In order to strengthen the anti-disturbance ability of the tracking control scheme, the fractional-order disturbance observer is developed to estimate the compound disturbance. To design a disturbance observer, the following auxiliary variable is introduced

$$e_i = \delta_i - r_i\xi_i, \tag{23}$$

whose differentiation is obtained from (19) as

$$\begin{cases} \mathcal{D}^{\nu}e_i = \mathcal{D}^{\nu}\delta_i - r_i\xi_{i+1} - \boldsymbol{\theta}_i^{*T}\boldsymbol{\vartheta}_i(\hat{\tilde{\boldsymbol{\xi}}}_i) - r_i(e_i + r_i\xi_i), \\ \mathcal{D}^{\nu}e_n = \mathcal{D}^{\nu}\delta_n - r_n u(v) - \boldsymbol{\theta}_n^{*T}\boldsymbol{\vartheta}_n(\hat{\tilde{\boldsymbol{\xi}}}_n) - r_n(e_n + r_n\xi_n), \end{cases} \tag{24}$$

in which $r_i > 0$ is design parameter of the developed disturbance observer.

To achieve the purpose of estimating the compound disturbance $\delta_i$, the estimation of the auxiliary variable $e_i$ should be obtained first. Thus, the following equations are given based on (24) as

$$\begin{cases} \mathcal{D}^{\nu}\hat{e}_i = -r_i\left(\hat{\xi}_{i+1} + \dfrac{1}{r_i}\hat{\boldsymbol{\theta}}_i^T\boldsymbol{\vartheta}_i(\hat{\tilde{\boldsymbol{\xi}}}_i) + \hat{e}_i + r_i\hat{\xi}_i\right), \\ \mathcal{D}^{\nu}\hat{e}_n = -r_n\left(u(v) + \dfrac{1}{r_n}\hat{\boldsymbol{\theta}}_n^T\boldsymbol{\vartheta}_n(\hat{\tilde{\boldsymbol{\xi}}}_n) + \hat{e}_n + r_n\hat{\xi}_n\right). \end{cases} \tag{25}$$

In the light of (23), one can get the estimation of $\delta_i$ as

$$\hat{\delta}_i = \hat{e}_i + r_i\hat{\xi}_i. \tag{26}$$

The estimation error of auxiliary variable is defined as $\tilde{e}_i = e_i - \hat{e}_i$. It follows from (23) and (26) that

$$\tilde{e}_i = \tilde{\delta}_i - r_i\tilde{\xi}_i. \tag{27}$$

Based on (24) and (25), the auxiliary error system is described as

$$\begin{cases} \mathcal{D}^{\nu}\tilde{e}_i = \mathcal{D}^{\nu}\delta_i - r_i\left(\tilde{\xi}_{i+1} + \dfrac{1}{r_i}\tilde{\boldsymbol{\theta}}_i^T\boldsymbol{\vartheta}_i(\hat{\tilde{\boldsymbol{\xi}}}_i) + \tilde{e}_i + r_i\tilde{\xi}_i\right), \\ \mathcal{D}^{\nu}\tilde{e}_n = \mathcal{D}^{\nu}\delta_n - r_n\left(\dfrac{1}{r_n}\tilde{\boldsymbol{\theta}}_n^T\boldsymbol{\vartheta}_n(\hat{\tilde{\boldsymbol{\xi}}}_n) + \tilde{e}_n + r_n\tilde{\xi}_n\right). \end{cases} \tag{28}$$

Consider the compound error system, which is composed of the state approximation error (21) and the auxiliary estimation error (28), the Lyapunov function candidate is chosen as

$$V_0(t) = \tilde{\boldsymbol{\xi}}^T\mathbf{P}\tilde{\boldsymbol{\xi}} + \frac{1}{2}\sum_{i=1}^{n}\tilde{e}_i^2. \tag{29}$$

According to Lemma 1, the $\nu$-th derivative of $V_0(t)$ can be expressed as

$$\begin{aligned} \mathcal{D}^{\nu}V_0(t) &\le (\mathcal{D}^{\nu}\tilde{\boldsymbol{\xi}})^T\mathbf{P}\tilde{\boldsymbol{\xi}} + \tilde{\boldsymbol{\xi}}^T\mathbf{P}(\mathcal{D}^{\nu}\tilde{\boldsymbol{\xi}}) + \sum_{i=1}^{n}\tilde{e}_i\mathcal{D}^{\nu}\tilde{e}_i \\ &= \tilde{\boldsymbol{\xi}}^T(\mathbf{A}^T\mathbf{P} + \mathbf{P}\mathbf{A})\tilde{\boldsymbol{\xi}} + 2\tilde{\boldsymbol{\xi}}^T\mathbf{P}(\tilde{\boldsymbol{\Theta}} + \tilde{\boldsymbol{\delta}}) - \sum_{i=1}^{n}r_i\tilde{e}_i^2 + \sum_{i=1}^{n}\tilde{e}_iD^{\nu}\delta_i \\ &\quad - \sum_{i=1}^{n-1}r_i\tilde{e}_i\tilde{\xi}_{i+1} - \sum_{i=1}^{n}r_i\tilde{e}_i\left(\frac{1}{r_i}\tilde{\boldsymbol{\theta}}_i^T\boldsymbol{\vartheta}_i(\hat{\tilde{\boldsymbol{\xi}}}_i) + r_i\tilde{\xi}_i\right). \end{aligned} \tag{30}$$

By employing the Young's inequality and (15), the following inequalities hold

$$\begin{cases} 2\tilde{\boldsymbol{\xi}}^T\mathbf{P}\tilde{\boldsymbol{\Theta}} \le \lambda_0 a_0^2\tilde{\boldsymbol{\xi}}^T(\mathbf{P}\mathbf{R}^{-1})^T\mathbf{P}\mathbf{R}^{-1}\tilde{\boldsymbol{\xi}} + \dfrac{1}{\lambda_0}\sum_{i=1}^{n}\tilde{\boldsymbol{\theta}}_i{}^T\tilde{\boldsymbol{\theta}}_i, \\ -\sum_{i=1}^{n}\tilde{e}_i\tilde{\boldsymbol{\theta}}_i^T\boldsymbol{\vartheta}_i(\hat{\tilde{\boldsymbol{\xi}}}_i) \le \dfrac{\lambda_0 a_0^2}{2}\tilde{\mathbf{e}}^T\tilde{\mathbf{e}} + \dfrac{1}{2\lambda_0}\sum_{i=1}^{n}\tilde{\boldsymbol{\theta}}_i{}^T\tilde{\boldsymbol{\theta}}_i, \end{cases} \tag{31}$$

where $a_0 = \max(a_i)$, $\tilde{\mathbf{e}} = [\tilde{e}_1, \tilde{e}_2, \cdots, \tilde{e}_n]^T$, $\mathbf{R} = \mathrm{diag}(r_1, r_2, \cdots, r_n)$ and $\lambda_0$ is design positive parameter.

It can be deduced from the Remark 2 that

$$\sum_{i=1}^{n}\tilde{e}_iD^{\nu}\delta_i \le \frac{1}{2}\tilde{\mathbf{e}}^T\tilde{\mathbf{e}} + \frac{1}{2}\bar{\boldsymbol{\delta}}^T\bar{\boldsymbol{\delta}}, \tag{32}$$

where $\bar{\boldsymbol{\delta}} = [\bar{\delta}_1, \bar{\delta}_2, \cdots, \bar{\delta}_n]^T$.

Denote $\boldsymbol{\Lambda} = [\tilde{\boldsymbol{\xi}}^T, \tilde{\mathbf{e}}^T]$. With (31) and (32), the derivative of $V_0$ is calculated as

$$\begin{aligned} \mathcal{D}^{\nu}V_0(t) \le -\boldsymbol{\Lambda}\begin{pmatrix} \mathbf{Q} - \lambda_0 a_0^2(\mathbf{P}\mathbf{R}^{-1})^T\mathbf{P}\mathbf{R}^{-1} - 2\mathbf{P}\mathbf{R} & -\mathbf{P} + \frac{1}{2}\mathbf{R}^T\mathbf{R} + \frac{\mathbf{R}}{2} \\ -\mathbf{P} + \frac{1}{2}\mathbf{R}^T\mathbf{R} + \frac{\mathbf{R}}{2} & \mathbf{R} - \frac{\lambda_0 + \lambda_0^2 a_0^2}{2\lambda_0}\mathbf{I}_{n\times n} \end{pmatrix}\boldsymbol{\Lambda}^T \\ + \frac{3}{2\lambda_0}\sum_{i=0}^{n}\tilde{\boldsymbol{\theta}}_i{}^T\tilde{\boldsymbol{\theta}}_i + \frac{1}{2}\bar{\boldsymbol{\delta}}^T\bar{\boldsymbol{\delta}}. \end{aligned} \tag{33}$$

*Remark 3* For the proposed nonlinear state observer, the appropriate approximation performance can be obtained by adjusting the design parameter $m_i$. Moreover, to make the state estimation follow the original system state rapidly, the bandwidth of the state observer should be designed to be greater than the bandwidth of the controller. In addition, in order to make $\tilde{\boldsymbol{\theta}}_i$ bounded, it is necessary to design an efficient controller.

### 3.2 Control design and stability analysis

In this part, an adaptive neural output feedback controller will be constructed by using the above composite observer and the backstepping technique. In order to overcome the input saturation constraint of the actuator, a dynamical auxiliary system of (34) is constructed to compensate for the effect of the saturation with the same order:

$$\begin{cases} \mathcal{D}^{\nu}\psi_i = \psi_{i+1} - \kappa_i\psi_i, 1 \leq i \leq n-1 \\ \mathcal{D}^{\nu}\psi_n = \Delta u - \kappa_n\psi_n, \end{cases} \tag{34}$$

where $\kappa_i$ is a positive design parameter that meets the specific condition to be determined later, and $\psi_i$ is state variable of the auxiliary system (34). Based on the controllable situation of the system (17) and Remark 1, $\Delta u$ can be considered as a bounded function, that is $|\Delta u| \leq \bar{u}$.

After incorporating the saturation error compensation signal, error variables are given as

$$\begin{cases} z_1 = \xi_1 - \psi_1 - y_d, \\ z_i = \hat{\xi}_i - \alpha_i^c - \psi_i. \end{cases} \tag{35}$$

In order to avoid the tedious analytic computation of the virtual control law, which results in the explosion of complexity in the sequel steps, a DSC is adopted to estimate the derivative of the virtual control law $\alpha_{i-1}$ as

$$\begin{cases} \varpi_i \mathcal{D}^{\nu}\alpha_i^c + \alpha_i^c = \alpha_{i-1}, \\ \alpha_i^c(0) = \alpha_{i-1}(0), \end{cases} \tag{36}$$

where $\varpi_i$ is positive constant, $z_i$ is called an error surface, and $\alpha_i^c$ is a state variable which is obtained by letting intermediate control function $\alpha_{i-1}$ pass through the fractional-order filter with a constant $\omega_i$. Define the output error of fractional-order filter $\chi_i = \alpha_i^c - \alpha_{i-1} (i = 2, \cdots, n)$. In the light of (35), one has

$$\hat{\xi}_i = z_i + \alpha_i^c + \psi_i = z_i + \chi_i + \alpha_{i-1} + \psi_i. \tag{37}$$

The $\nu$-th Caputo derivative of $\chi_i$ can be obtained as

$$\mathcal{D}^{\nu}\chi_i = \mathcal{D}^{\nu}\alpha_i^c - \mathcal{D}^{\nu}\alpha_{i-1} = -\frac{\chi_i}{\varpi_i} + H_i, \tag{38}$$

where $H_i$ is a continuous function of variables $z_1, \cdots, z_i, \chi_2, \cdots, \chi_i, \hat{\boldsymbol{\theta}}_1, \cdots, \hat{\boldsymbol{\theta}}_i$, $\hat{\delta}_1, \cdots, \hat{\delta}_i$, $y_d$, $\mathcal{D}^{\nu}y_d$ and $\mathcal{D}^{\nu}(\mathcal{D}^{\nu}y_d)$.

*Remark 4* From (34), it should be emphasized that the error $\Delta u = u(v) - v$ is the input of the auxiliary system, and the upper bound of $|y - y_d|$ relies on the upper bound of $\Delta u$ and design parameters. In the case of no input saturation, that is, $\Delta u = 0$, the value of the variable $\psi_i$ is very tiny, and it does not affect the design of the controller. In the presence of the input saturation, the auxiliary system (34) can be activated so that the variable $\psi_i$ is used to modify the tracking error $z_1$ to compensate for the input saturation. Therefore, the mentioned auxiliary system can effectively solve the input saturation problem.

*Remark 5* By Assumption 1 and the property of continuous function, one has $\Xi_0 = \left\{(y_d, \mathcal{D}^\nu y_d, \mathcal{D}^\nu(\mathcal{D}^\nu y_d)) : (y_d)^2 + (\mathcal{D}^\nu y_d)^2 + (\mathcal{D}^\nu(\mathcal{D}^\nu y_d))^2 \leq \eta_0\right\}$ is compact, where $\eta_0$ is a positive constant. In addition, there exists a positive constant $\eta_i$ such that the set $\Xi_i = \left\{\sum_{\imath=1}^{i}(z_i^2 + \frac{1}{\gamma_i}\tilde{\boldsymbol{\theta}}_i^T\tilde{\boldsymbol{\theta}}_i + \psi_i^2 + e_i^2) + \sum_{\imath=1}^{i-1}\chi_{i+1}^2 + \tilde{\boldsymbol{\xi}}_i^T\mathbf{P}_i\tilde{\boldsymbol{\xi}}_i \leq 2\eta_i\right\}$ is also compact. From the obtained results [19, 35], one has $|H_i| \leq \bar{h}_i$ $(i = 2, \cdots, n)$ under the compact set $\Xi_0 \times \Xi_i$, where $\bar{h}_i$ is the upper bound of $H_i$.

The detailed design process is given as follows.

Step 1. From (19), (34) and (35), the $\nu$-th fractional-order derivative of $z_1$ is

$$\begin{aligned}\mathcal{D}^\nu z_1 &= \mathcal{D}^\nu\xi_1 - \mathcal{D}^\nu\psi_1 - \mathcal{D}^\nu y_d\\ &= \xi_2 + \frac{1}{r_1}\boldsymbol{\theta}_1^{*T}\boldsymbol{\vartheta}_1(\hat{\xi}_1) + \delta_1 - (\psi_2 - \kappa_1\psi_1) - \mathcal{D}^\nu y_d\\ &= \tilde{\xi}_2 + z_2 + \chi_2 + \alpha_1 + \psi_2 + \frac{1}{r_1}\boldsymbol{\theta}_1^{*T}\boldsymbol{\vartheta}_1(\hat{\xi}_1) + \delta_1 + \kappa_1\psi_1 - \psi_2 - \mathcal{D}^\nu y_d\\ &= \tilde{\xi}_2 + z_2 + \chi_2 + \alpha_1 + \frac{1}{r_1}\boldsymbol{\theta}_1^{*T}\boldsymbol{\vartheta}_1(\hat{\xi}_1) + \delta_1 + \kappa_1\psi_1 - \mathcal{D}^\nu y_d,\end{aligned} \tag{39}$$

where $\alpha_1$ is the designed virtual control law. Then, the first virtual control law $\alpha_1$ is constructed as

$$\alpha_1 = -\left(k_1 + \frac{3}{2}\right)z_1 - \frac{1}{r_1}\hat{\boldsymbol{\theta}}_1^T\boldsymbol{\vartheta}_1(\hat{\xi}_1) - \hat{\delta}_1 - \kappa_1\psi_1 + \mathcal{D}^\nu y_d, \tag{40}$$

where $k_1 > 0$ is the design parameter. Furthermore, the fractional adaptive law for $\mathcal{D}^\nu\hat{\boldsymbol{\theta}}_1$ is chosen as

$$\mathcal{D}^\nu\hat{\boldsymbol{\theta}}_1 = \gamma_1\left(\frac{1}{r_1}z_1\boldsymbol{\vartheta}_1(\hat{\xi}_1) - \mu_1\hat{\boldsymbol{\theta}}_1\right), \tag{41}$$

where $\gamma_1, \mu_1 > 0$ are design constants. Substituting (40) into (39) yields

$$\mathcal{D}^\nu z_1 = -\left(k_1 + \frac{3}{2}\right)z_1 + z_2 + \chi_2 + \tilde{\xi}_2 + \frac{1}{r_1}\tilde{\boldsymbol{\theta}}_1^T\boldsymbol{\vartheta}_1(\hat{\xi}_1) + \tilde{\delta}_1. \tag{42}$$

According to (34) and the Young's inequality, the following inequalities are presented

$$\begin{cases} \psi_1 \mathcal{D}^\nu \psi_1 = -\kappa_1 \psi_1^2 + \psi_1 \psi_2 \leq -\left(\kappa_1 - \frac{1}{2}\right) \psi_1^2 + \frac{1}{2}\psi_2^2, \\ z_1(\tilde{\xi}_2 + \tilde{\delta}_1) = z_1(\tilde{\xi}_2 + \tilde{e}_1 + r_1 \tilde{\xi}_1) \leq \frac{3}{2} z_1^2 + \frac{1}{2}\tilde{e}_1^2 + \frac{r_1^2}{2}\tilde{\xi}_1^2 + \frac{1}{2}\tilde{\xi}_2^2. \end{cases} \tag{43}$$

Considering the error signals $z_1$, $\tilde{\boldsymbol{\theta}}_1$ and $\psi_1$, the Layapunov function is chosen as

$$V_1(t) = \frac{1}{2} z_1^2 + \frac{1}{2\gamma_1} \tilde{\boldsymbol{\theta}}_1^T \tilde{\boldsymbol{\theta}}_1 + \frac{1}{2}\psi_1^2. \tag{44}$$

The $\nu$-th derivative of $V_1(t)$ can be described as

$$\begin{aligned} \mathcal{D}^\nu V_1(t) &\leq z_1 \mathcal{D}^\nu z_1 + \frac{1}{\gamma_1} \tilde{\boldsymbol{\theta}}_1^T \mathcal{D}^\nu \tilde{\boldsymbol{\theta}}_1 + \psi_1 \mathcal{D}^\nu \psi_1 \\ &\leq -\left(k_1 + \frac{3}{2}\right) z_1^2 + z_1 z_2 + \tilde{\boldsymbol{\theta}}_1^T \left(\frac{1}{r_1} z_1 \boldsymbol{\vartheta}_1(\hat{\xi}_1) - \frac{1}{\gamma_1} \mathcal{D}^\nu \hat{\boldsymbol{\theta}}_1\right) \\ &\quad + z_1(\tilde{\xi}_2 + \tilde{\delta}_1) + z_1 \chi_2 - \left(\kappa_1 - \frac{1}{2}\right) \psi_1^2 + \frac{1}{2}\psi_2^2 \\ &\leq -k_1 z_1^2 + z_1 z_2 + \frac{1}{2}\tilde{e}_1^2 + \frac{r_1^2}{2}\tilde{\xi}_1^2 + \frac{1}{2}\tilde{\xi}_2^2 - \frac{\mu_1}{2}\tilde{\boldsymbol{\theta}}_1^T \tilde{\boldsymbol{\theta}}_1 + \frac{\mu_1}{2}\boldsymbol{\theta}_1^{*T} \boldsymbol{\theta}_1^* \\ &\quad + z_1 \chi_2 - \left(\kappa_1 - \frac{1}{2}\right) \psi_1^2 + \frac{1}{2}\psi_2^2, \end{aligned} \tag{45}$$

where $z_1 z_2$ will be tackled in the next step.

Step $i$ ($i = 2, \cdots, n-1$): Similar with (39) in Step 1, differentiating $z_i$ with respect to time yields

$$\begin{aligned} \mathcal{D}^\nu z_i &= \mathcal{D}^\nu \hat{\xi}_i - \mathcal{D}^\nu \psi_i - \mathcal{D}^\nu \alpha_i^c \\ &= \hat{\xi}_{i+1} + \frac{1}{r_i} \hat{\boldsymbol{\theta}}_i^T \boldsymbol{\vartheta}_i(\hat{\bar{\boldsymbol{\xi}}}_i) + m_i(y - \hat{\xi}_1) + \hat{\delta}_i - (\psi_{i+1} - \kappa_i \psi_i) - \mathcal{D}^\nu \alpha_i^c \\ &= z_{i+1} + \chi_{i+1} + \alpha_i + \frac{1}{r_i} \hat{\boldsymbol{\theta}}_i^T \boldsymbol{\vartheta}_i(\hat{\bar{\boldsymbol{\xi}}}_i) + m_i(y - \hat{\xi}_1) + \hat{\delta}_i + \kappa_i \psi_i - \mathcal{D}^\nu \alpha_i^c, \end{aligned} \tag{46}$$

where $\alpha_i$ is the virtual control law. Design the $i$-th intermediate control function $\alpha_i$ and the fractional adaptive law as

$$\begin{cases} \alpha_i = -k_i z_i - z_{i-1} - \frac{1}{r_i} \hat{\boldsymbol{\theta}}_i \boldsymbol{\vartheta}_i(\hat{\bar{\boldsymbol{\xi}}}_i) - m_i(y - \hat{\xi}_1) - \hat{\delta}_i - \kappa_i \psi_i + \mathcal{D}^\nu \alpha_i^c, \\ \mathcal{D}^\nu \hat{\boldsymbol{\theta}}_i = \gamma_i (z_i \boldsymbol{\vartheta}_i(\hat{\bar{\boldsymbol{\xi}}}_i) - \mu_i \hat{\boldsymbol{\theta}}_i), \end{cases} \tag{47}$$

where $k_i$, $\gamma_i$ and $\mu_i$ are positive constants. Substituting (47) into (46) results in

$$\mathcal{D}^\nu z_i = -k_i z_i + z_{i+1} - z_{i-1} + \chi_{i+1}. \tag{48}$$

On the basis of (34) and the Young's inequality, the following inequality can be obtained

$$\psi_i \mathcal{D}^\nu \psi_i = -\kappa_i \psi_i^2 + \psi_i \psi_{i+1} \leq -\left(\kappa_i - \frac{1}{2}\right)\psi_i^2 + \frac{1}{2}\psi_{i+1}^2. \tag{49}$$

Construct the following Layapunov function candidate

$$V_i(t) = \frac{1}{2}z_i^2 + \frac{1}{2\gamma_i}\tilde{\boldsymbol{\theta}}_i^T\tilde{\boldsymbol{\theta}}_i + \frac{1}{2}\psi_i^2 + \frac{1}{2}\chi_i^2. \tag{50}$$

Invoking (47), (49) and (50), one has

$$\begin{aligned}
\mathcal{D}^\nu V_i(t) &\leq z_i \mathcal{D}^\nu z_i + \frac{1}{\gamma_i}\tilde{\boldsymbol{\theta}}_i^T \mathcal{D}^\nu \tilde{\boldsymbol{\theta}}_i + \psi_i \mathcal{D}^\nu \psi_i + \chi_i \mathcal{D}^\nu \chi_i \\
&\leq -k_i z_i^2 + z_i z_{i+1} - z_{i-1} z_i + z_i \chi_{i+1} + \chi_i \mathcal{D}^\nu \chi_i \\
&\quad - \frac{1}{\gamma_i}\tilde{\boldsymbol{\theta}}_i^T \mathcal{D}^\nu \hat{\boldsymbol{\theta}}_i - \left(\kappa_i - \frac{1}{2}\right)\psi_i^2 + \frac{1}{2}\psi_{i+1}^2 \\
&\leq -\left(k_i - \frac{1}{2}\lambda_i a_i^2\right) z_i^2 + z_i z_{i+1} - z_{i-1} z_i + z_i \chi_{i+1} + \chi_i \left[-\frac{\chi_i}{\varpi_i} + H_i\right] \\
&\quad - \left(\frac{\mu_i}{2} - \frac{1}{2\lambda_i}\right)\tilde{\boldsymbol{\theta}}_i^T \tilde{\boldsymbol{\theta}}_i + \frac{\mu_i}{2}\boldsymbol{\theta}_i^{*T}\boldsymbol{\theta}_i^* - \left(\kappa_i - \frac{1}{2}\right)\psi_i^2 + \frac{1}{2}\psi_{i+1}^2,
\end{aligned} \tag{51}$$

where $\lambda_i > 0$ and $z_i z_{i+1}$ will be canceled in the next step.

Step $n$: In the final step, from (20), (34) and (35), one can obtain

$$\begin{aligned}
\mathcal{D}^\nu z_n &= \mathcal{D}^\nu \hat{\xi}_n - \mathcal{D}^\nu \psi_n - \mathcal{D}^\nu \alpha_n^c \\
&= u(v) + \frac{1}{r_n}\hat{\boldsymbol{\theta}}_n^T \boldsymbol{\vartheta}_n(\hat{\bar{\boldsymbol{\xi}}}_n) + m_n(y - \hat{\xi}_1) + \hat{\delta}_n - (\Delta u - \kappa_n \psi_n) - \mathcal{D}^\nu \alpha_n^c \\
&= v + \frac{1}{r_n}\hat{\boldsymbol{\theta}}_n^T \boldsymbol{\vartheta}_n(\hat{\bar{\boldsymbol{\xi}}}_n) + m_n(y - \hat{\xi}_1) + \hat{\delta}_n + \kappa_n \psi_n - \mathcal{D}^\nu \alpha_n^c,
\end{aligned} \tag{52}$$

where $v$ is the actual control input. The desired actual control signal $v$ and adaptive law can be respectively constructed as

$$\begin{cases}
v = -k_n z_n - z_{n-1} - \dfrac{1}{r_n}\hat{\boldsymbol{\theta}}_n^T \boldsymbol{\vartheta}_n(\hat{\bar{\boldsymbol{\xi}}}_n) - m_n(y - \hat{\xi}_1) - \hat{\delta}_n - \kappa_n \psi_n + \mathcal{D}^\nu \alpha_n^c, \\
\mathcal{D}^\nu \hat{\boldsymbol{\theta}}_n = \gamma_n(z_n \boldsymbol{\vartheta}_n(\hat{\bar{\boldsymbol{\xi}}}_n) - \mu_n \hat{\boldsymbol{\theta}}_n),
\end{cases} \tag{53}$$

where $k_n$, $\gamma_n$ and $\mu_n$ are positive parameters. Substituting (53) into (52) yields

$$\mathcal{D}^\nu z_n = -k_n z_n - z_{n-1}. \tag{54}$$

Similar to the derivation process of (43) and (49), the following formula is established as

$$\psi_n \mathcal{D}^\nu \psi_n = -\kappa_n \psi_n^2 + \psi_n \Delta u \leq -\left(\kappa_n - \frac{1}{2}\right)\psi_n^2 + \frac{1}{2}\bar{u}^2. \tag{55}$$

The Layapunov function is chosen as

$$V_n(t) = \frac{1}{2}z_n^2 + \frac{1}{2\gamma_n}\tilde{\boldsymbol{\theta}}_n^T\tilde{\boldsymbol{\theta}}_n + \frac{1}{2}\psi_n^2 + \frac{1}{2}\chi_n^2. \tag{56}$$

By applying Lemma 1, (53), (54) and (55), the Caputo derivative of $V_n(t)$ can be rewritten as

$$\begin{aligned}
\mathcal{D}^\nu V_n(t) &\leq z_n\mathcal{D}^\nu z_n + \frac{1}{\gamma_n}\tilde{\boldsymbol{\theta}}_n^T\mathcal{D}^\nu\tilde{\boldsymbol{\theta}}_n + \psi_n\mathcal{D}^\nu\psi_n + \chi_n\mathcal{D}^\nu\chi_n \\
&\leq -k_n z_n^2 - z_n z_{n-1} - \frac{1}{\gamma_n}\tilde{\boldsymbol{\theta}}_n^T\mathcal{D}^\nu\hat{\boldsymbol{\theta}}_n - \left(\kappa_n - \frac{1}{2}\right)\psi_n^2 + \frac{1}{2}\bar{u}^2 + \chi_n\mathcal{D}^\nu\chi_n \\
&\leq -\left(k_n - \frac{1}{2}\lambda_n a_n^2\right)z_n^2 - z_n z_{n-1} - \left(\frac{\mu_n}{2} - \frac{1}{2\lambda_n}\right)\tilde{\boldsymbol{\theta}}_n^T\tilde{\boldsymbol{\theta}}_n + \frac{\mu_n}{2}\boldsymbol{\theta}_n^{*T}\boldsymbol{\theta}_n^* \\
&\quad - \left(\kappa_n - \frac{1}{2}\right)\psi_n^2 + \frac{1}{2}\bar{u}^2 + \chi_n\left[-\frac{\chi_n}{\varpi_n} + H_n\right].
\end{aligned} \tag{57}$$

The above design procedure of the composite observer-based adaptive neural control can be shown in the following theorem, which contains the result of adaptive control scheme for the FONS in the presence of input saturation and external disturbance using the backstepping technique.

**Theorem 1** *Consider the FONS* (12) *under Assumptions 1-3 subject to the input saturation and external disturbance. The state observer is designed as* (20)*, the disturbance observer is designed in accordance with* (26)*, the adaptive control law is chosen as* (53)*, and the updated laws of the neural networks are chosen as* (41), (47) *and* (53)*. Then, there exist appropriate design parameters* $m_i$*,* $r_i$*,* $k_i$*,* $\kappa_i$*,* $\varpi_i$ *and* $\mu_i$ *such that whole closed loop signals are bounded. Furthermore, the tracking error signal* $z_1$ *converges to a small neighborhood of the origin.*

**Proof.** The entire Lyapunov function is considered as

$$V(t) = V_0(t) + \sum_{i=1}^{n} V_i(t). \tag{58}$$

Substituting (45), (51) and (57) into (58) results in

$$\begin{aligned}
\mathcal{D}^\nu V(t) &= \mathcal{D}^\nu V_0(t) + \mathcal{D}^\nu\sum_{i=1}^{n} V_i(t) \\
&\leq \mathcal{D}^\nu V_0(t) - k_1 z_1^2 - \sum_{i=2}^{n}\left(k_i - \frac{1}{2}\lambda_i a_i^2\right)z_i^2 - \frac{\mu_1}{2}\tilde{\boldsymbol{\theta}}_1^T\tilde{\boldsymbol{\theta}}_1 + \sum_{i=1}^{n}\frac{\mu_i}{2}\boldsymbol{\theta}_i^{*T}\boldsymbol{\theta}_i^* \\
&\quad - \sum_{i=2}^{n}\left(\frac{\mu_i}{2} - \frac{1}{2\lambda_i}\right)\tilde{\boldsymbol{\theta}}_i^T\tilde{\boldsymbol{\theta}}_i - \left(\kappa_1 - \frac{1}{2}\right)\psi_1^2 - \sum_{i=2}^{n}(\kappa_i - 1)\psi_i^2 + \frac{1}{2}\bar{u}^2 \\
&\quad + \sum_{i=1}^{n-1} z_i\chi_{i+1} + \sum_{i=1}^{n-1}\chi_{i+1}\left(-\frac{\chi_{i+1}}{\varpi_{i+1}} + H_{i+1}\right) + \frac{1}{2}\tilde{e}_1^2 + \frac{r_1^2}{2}\tilde{\xi}_1^2 + \frac{1}{2}\tilde{\xi}_2^2.
\end{aligned} \tag{59}$$

Then, one has

$$\begin{aligned}\mathcal{D}^{\nu}V(t) \leq & -\boldsymbol{\Lambda}\begin{pmatrix}\mathbf{Q}-\lambda_0 a_0^2(\mathbf{P}\mathbf{R}^{-1})^T\mathbf{P}\mathbf{R}^{-1}-2\mathbf{P}\mathbf{R}-\mathbf{R}_1 & -\mathbf{P}+\frac{\mathbf{R}^T\mathbf{R}}{2}+\frac{\mathbf{R}}{2}\\ -\mathbf{P}+\frac{\mathbf{R}^T\mathbf{R}}{2}+\frac{\mathbf{R}}{2} & \mathbf{R}-\frac{\lambda_0+\lambda_0^2 a_0^2}{2\lambda_0}\mathbf{I}_{n\times n}-\mathbf{E}_1\end{pmatrix}\boldsymbol{\Lambda}^T+\frac{1}{2}\bar{u}^2\\ & -\left(k_1-\frac{1}{2}\right)z_1^2-\sum_{i=2}^{n}\left(k_i-\frac{1}{2}-\frac{1}{2}\lambda_i a_i^2\right)z_i^2-\left(\frac{\mu_1}{2}-\frac{3}{2\lambda_0}\right)\tilde{\boldsymbol{\theta}}_1^T\tilde{\boldsymbol{\theta}}_1\\ & -\sum_{i=2}^{n}\left(\frac{\mu_i}{2}-\frac{1}{2\lambda_i}-\frac{3}{2\lambda_0}\right)\tilde{\boldsymbol{\theta}}_i^T\tilde{\boldsymbol{\theta}}_i-\left(\kappa_1-\frac{1}{2}\right)\psi_1^2-\sum_{i=2}^{n}(\kappa_i-1)\psi_i^2\\ & -\sum_{i=1}^{n-1}\left[\frac{1}{\varpi_{i+1}}-\frac{1}{2}-\frac{\bar{\hbar}_i}{2\sigma_i}\right]\chi_{i+1}^2+\sum_{i=1}^{n}\frac{\mu_i}{2}\boldsymbol{\theta}_i^{*T}\boldsymbol{\theta}_i^*+\frac{1}{2}\bar{\boldsymbol{\delta}}^T\bar{\boldsymbol{\delta}}+\sum_{i=1}^{n-1}2\sigma_i,\end{aligned} \tag{60}$$

where $\mathbf{R}_1=\mathrm{diag}(\frac{r_1^2}{2},\frac{1}{2},0,\cdots,0)$, $\mathbf{E}_1=\mathrm{diag}(\frac{1}{2},0,\cdots,0)$, $\sigma_i>0$. Denote $\mathbf{G}=\begin{pmatrix}(\mathbf{Q}-\lambda_0 a_0^2(\mathbf{P}\mathbf{R}^{-1})^T\mathbf{P}\mathbf{R}^{-1}-2\mathbf{P}\mathbf{R}-\mathbf{R}_1)\mathbf{P}^{-1} & (-\mathbf{P}+\frac{\mathbf{R}^T\mathbf{R}}{2}+\frac{\mathbf{R}}{2})\mathbf{P}^{-1}\\ 2(-\mathbf{P}+\frac{\mathbf{R}^T\mathbf{R}}{2}+\frac{\mathbf{R}}{2}) & 2\left(\mathbf{R}-\frac{\lambda_0+\lambda_0^2 a_0^2}{2\lambda_0}\mathbf{I}_{n\times n}-\mathbf{E}_1\right)\end{pmatrix}$, $\rho=\min\left\{\lambda_{min}(\mathbf{G}),2k_1-1,2k_i-1-\lambda_i a_i^2,\gamma_1\left(\mu_1-\frac{3}{\lambda_0}\right),\gamma_i\left(\mu_i-\frac{1}{\lambda_i}-\frac{3}{\lambda_0}\right),2\kappa_1-1,2\kappa_i-2,\frac{2}{\varpi_i}-1-\frac{\bar{\hbar}_i}{\sigma_i}\right\}$ and $\Upsilon=\sum_{i=1}^{n}\frac{\mu_i}{2}\boldsymbol{\theta}_i^{*T}\boldsymbol{\theta}_i^*+\frac{1}{2}\bar{\boldsymbol{\delta}}^T\bar{\boldsymbol{\delta}}+\frac{1}{2}\bar{u}^2+\sum_{i=1}^{n-1}2\sigma_i$. To guarantee the stability of the closed loop system, the corresponding design parameters $\mathbf{G}$, $\varpi_i$, $k_i$, $\mu_i$ and $\kappa_i$ should be chosen to make the following inequalities hold

$$\begin{cases}\mathbf{G}>0,\\ k_1-\dfrac{1}{2}>0,\\ k_i-\dfrac{1}{2}-\dfrac{\lambda_i a_i^2}{2}>0,\\ \dfrac{\mu_1}{2}-\dfrac{3}{2\lambda_0}>0,\\ \dfrac{\mu_i}{2}-\dfrac{1}{2\lambda_i}-\dfrac{3}{2\lambda_0}>0,\\ \dfrac{1}{\varpi_i}-\dfrac{1}{2}-\dfrac{\bar{\hbar}_i}{2\sigma_i}>0,\\ \kappa_1-\dfrac{1}{2}>0,\\ \kappa_i-1>0.\end{cases} \tag{61}$$

Then, it can be obtained

$$\mathcal{D}^{\nu}V(t)\leq -\rho V(t)+\Upsilon. \tag{62}$$

According to Lemma 4, (62) can be rewritten as

$$V(t)\leq V(0)E_{\nu}(-\rho t^{\nu})+\frac{\epsilon\Upsilon}{\rho}, \tag{63}$$

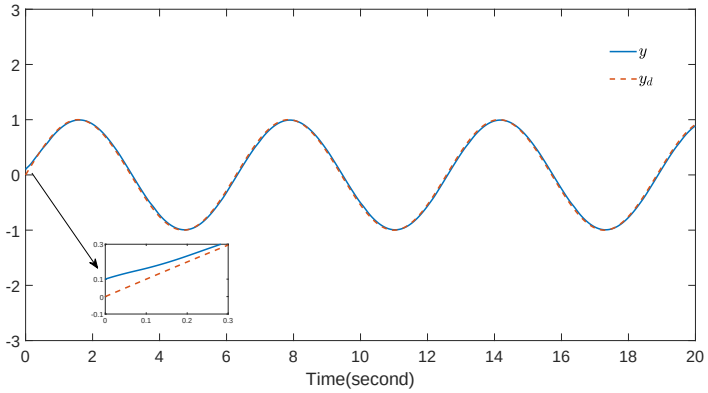


**Fig. 1** Output $y(t)$ follows desired trajectory $y_d(t)$.

Then, one has

$$\lim_{t\to\infty} |V(t)| \leq \frac{\epsilon\Upsilon}{\rho}. \tag{64}$$

By Lemma 4 and the definition of $V(t)$, it can be concluded that the boundedness of the FONS (12) is obtained, and the tracking error can converge to a small neighborhood of the origin $|z_1(t)| \leq \sqrt{\frac{2\epsilon\Upsilon}{\rho}}$ by choosing the appropriate parameters. This concludes the proof.

*Remark 6* In this paper, the DSC scheme using the state observer and the disturbance observer is designed for a strict feedback the FONSs with unknown functions, external disturbances, input saturation and unmeasurable states. In order to achieve an accurate estimation of the unmeasurable states, a fractional-order disturbance observer is constructed to estimate disturbances, and the output of disturbance observer is used to construct the controller, as shown in (40), (47) and (53). In addition, a signal $\psi_i$ is introduced at each step of the above mentioned backstepping design to compensate for the effect of saturation constraint, and this signal is also used to design an adaptive neural controller.

## 4 Simulation results

In this section, simulation results of two examples are presented to show the feasibility and the applicability of our developed adaptive neural output feedback control method, and it is assumed that there is no prior information about the nonlinearity and state of the system except for the feedback output.

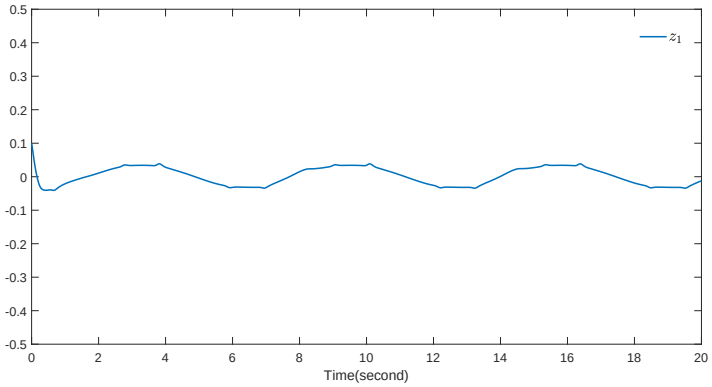


**Fig. 2** The tracking error $z_1(t)$.

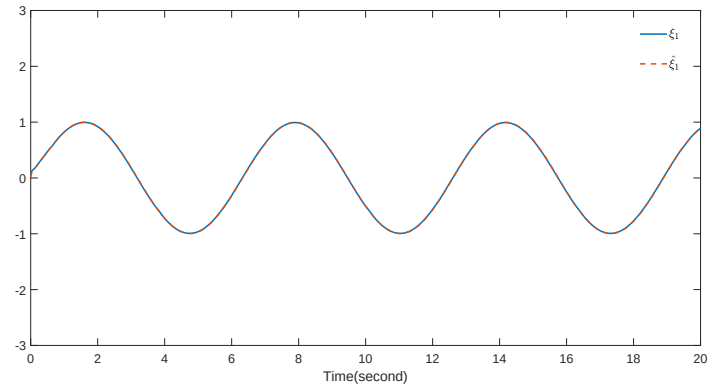


**Fig. 3** Trajectories of $\xi_1(t)$ and $\hat{\xi}_1(t)$.

### 4.1 Example 1

Consider a fractional-order nonlinear system in the presence of input saturation and unknown external disturbance as

$$\begin{cases} \mathcal{D}^{\nu}\xi_1 = \xi_2 + f_1(\xi_1) + d_1(t), \\ \mathcal{D}^{\nu}\xi_2 = u(v) + f_2(\bar{\boldsymbol{\xi}}_2) + d_2(t), \\ y = \xi_1, \end{cases} \tag{65}$$

where $\nu = 0.95$, $f_1(\xi_1) = -0.02\xi_1^2$, $f_2(\bar{\boldsymbol{\xi}}_2) = \frac{\xi_2 - 0.3\xi_1^2}{1+\xi_1^2}$, $d_1(t) = 0.5\cos t$ and $d_2(t) = 0.5\sin t$.

For the control plant (65), the proposed adaptive neural feedback control approach with the controller (53) along with the adaptive update laws (41), (47) and (53) is employed to ensure accurate estimation of the state and realize

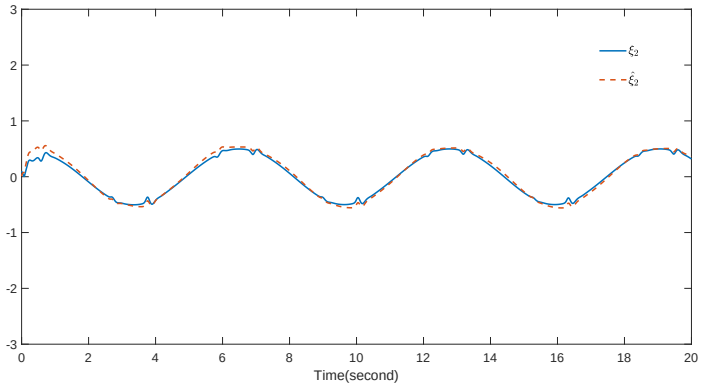


**Fig. 4** Trajectories of $\xi_2(t)$ and $\hat{\xi}_2(t)$.

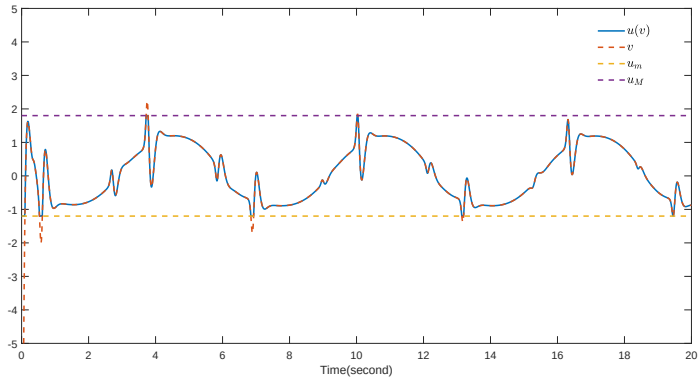


**Fig. 5** Trajectories of $u(v)$, $v$ and constraint interval.

signal tracking purpose, i.e., $y \to y_d$ $(t \to \infty)$, with the input saturation

$$u(v) = \begin{cases} 1.5, & v \geq 1.5, \\ v, & -1.8 < v < 1.5, \\ -1.8, & v \leq -1.8. \end{cases} \tag{66}$$

To verify the developed control scheme, Theorem 1 is applied to design the controller to render the output $y$ to track desired signal $y_d = \sin t$. The parameters in controller and adaptive laws are selected as $k_1 = 20$, $k_2 = 30$, $r_1 = 3.2$, $r_2 = 3.2$, $\gamma_1 = 15$, $\gamma_2 = 20$, $\mu_1 = 0.1$, $\mu_2 = 0.1$, $\kappa_1 = \kappa_2 = 5$, $\varpi_2 = 0.05$, $\lambda_0 = \lambda_1 = \lambda_2 = 200$, and the selection of parameters satisfy the conditions (61). Initial conditions of states are chosen as $\xi_1(0) = 0.1$, $\xi_2(0) = 0.1$, $\hat{\xi}_1(0) = 0.01$, $\hat{\xi}_2(0) = 0.01$ and $\psi_1(0) = \psi_2(0) = 0.01$. The neural network $\hat{\boldsymbol{\theta}}_1^T \boldsymbol{\varphi}(\hat{\xi}_1)$ contains 7 nodes with centers evenly distributed on $[-3, 3]$. Similarly, $\hat{\boldsymbol{\theta}}_2^T \boldsymbol{\varphi}(\hat{\bar{\boldsymbol{\xi}}}_2)$ contains $7^2$ nodes, with centers evenly spaced in

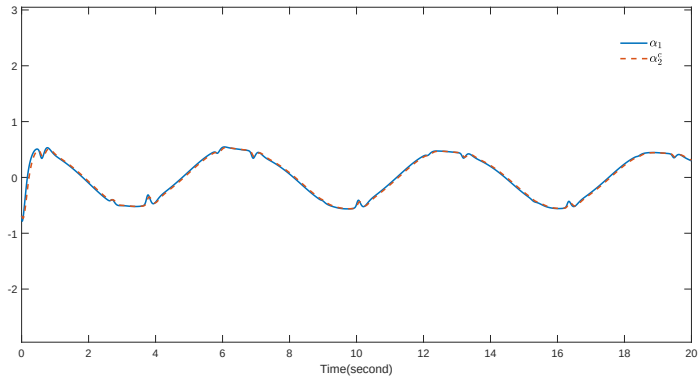


**Fig. 6** Trajectories of $\alpha_1$ and $\alpha_2^c$.

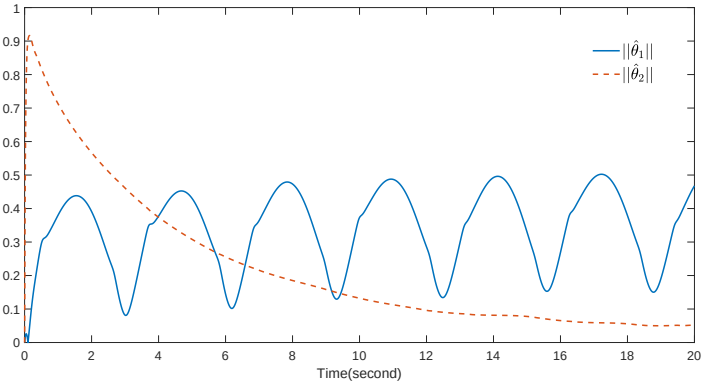


**Fig. 7** Parameters adaptive law $||\hat{\boldsymbol{\theta}}_1||$ and $||\hat{\boldsymbol{\theta}}_2||$.

$[-3,3] \times [-3,3]$. Let $m_1 = 30$, $m_2 = 40$, then it can be inferred that $\mathbf{A}$ is Hurwitz based on (22). By choosing $Q = 5I$, one has

$$\mathbf{P} = \begin{pmatrix} 0.25 & 0.015 \\ 0.015 & 0.25 \end{pmatrix},$$

and

$$\mathbf{G} = \begin{pmatrix} 13.21 & -1.98 & 6.47 & -0.015 \\ -2.34 & 38.94 & -0.015 & 6.62 \\ 6.47 & -0.015 & 3.4 & 0 \\ -0.015 & 6.62 & 0 & 4.4 \end{pmatrix},$$

which are positive definite matrixes.

The simulation results are given in Figs. 1-7. Fig. 1 shows the trajectory of the control output $y$ and the reference signal $y_d$ and Fig. 2 plots the tracking error, and it fluctuates within the interval $[-0.06, 0.06]$; Figs. 3-4 display the

trajectory of state $\xi_i$ and its estimation $\hat{\xi}_i$, $i = 1, 2$; The control input $v$ and the saturation control input $u(v)$ are described in Fig. 5; Fig. 6 shows the virtual control $\alpha_1$ and the filter output $\alpha_2^c$. The norm of parameters estimation of the neural network is shown in Fig. 7. From these results, it can be concluded that the proposed method can effectively tackle the uncertain FONSs subject to the unmeasurable state, input saturation and unknown disturbance, and the control performance is satisfactory.

### 4.2 Example 2

The following fractional-order Arneodo chaotic system is considered [36]

$$\begin{cases} \mathcal{D}^{\nu}\xi_1(t) = \xi_2, \\ \mathcal{D}^{\nu}\xi_2(t) = \xi_3, \\ \mathcal{D}^{\nu}\xi_3(t) = u(v) + f_3(\bar{\boldsymbol{\xi}}_3) + d_3(t), \end{cases} \tag{67}$$

where the system order is $\nu = 0.98$, the corresponding unknown nonlinear functions are presented as $f_1(\xi_1) = 0$, $f_2(\bar{\boldsymbol{\xi}}_2) = 0$, $f_3(\bar{\boldsymbol{\xi}}_3) = 2\xi_1 - \xi_2 - \xi_3 - \xi_1^3$, and the unknown time varying disturbances are given by $d_1(t) = 0$, $d_2(t) = 0$, $d_3(t) = \sin t$. Initial conditions are chosen as $\bar{\boldsymbol{\xi}}_{\mathbf{3}} = [-0.2, 0.1, 0.1]^T$, $\hat{\bar{\boldsymbol{\xi}}}_{\mathbf{3}} = [0.1, 0.1, 0.1]^T$, $\psi_1(0) = \psi_2(0) = \psi_3(0) = 0.01$ and the other initial values are selected as zeros. The input saturation $u(v)$ is expressed by (13), where $u_M = 23$ and $u_m = -15$. The desired reference signal is chosen as $y_d = \sin t$. Choose design parameters as $\kappa_1 = \kappa_2 = \kappa_3 = 5$, $r_1 = r_2 = 2.8$, $r_3 = 2.3$, $k_1 = 15$, $k_2 = 20$, $k_3 = 25$, $\gamma_3 = 10$, $\mu_3 = 0.05$, $\varpi_2 = \varpi_3 = 0.05$. Similar with Example 4.1, select the gain parameters as $m_1 = 10$, $m_2 = 110$, $m_3 = 300$, then one has

$$\mathbf{P} = \begin{pmatrix} 0.645 & 0.06 & -0.3 \\ 0.06 & 0.656 & -0.0004 \\ -0.3 & -0.0004 & 0.668 \end{pmatrix},$$

and

$$\mathbf{G} = \begin{pmatrix} 12.55 & -1.14 & 5.64 & 4.68 & -0.06 & 0.3 \\ -1.04 & 8.89 & -0.46 & -0.06 & 4.66 & 0.0004 \\ 6.09 & -0.55 & 12.98 & 0.3 & 0.004 & 3.13 \\ 4.68 & -0.06 & 0.3 & 2.6 & 0 & 0 \\ -0.06 & 4.66 & 0.0004 & 0 & 3.6 & 0 \\ 0.3 & 0.004 & 3.13 & 0 & 0 & 2.6 \end{pmatrix},$$

which are positive definite matrixes.

Figs. 8-10 display the simulation results of Example 2. The chaotic behaviour of the fractional-order Arneodo system is shown in Fig. 8 when $u(v) = 0$ and $d_3(t) = 0$. The tracking control result of the uncertain fractional-order system is displayed in Fig. 9, which displays a satisfactory tracking performance and ensure that the tracking error converges to the interval $[-0.08, 0.08]$ after $4s$, and the trajectories of state $\xi_i$ and its estimation $\hat{\xi}_i$ are given, $i = 1, 2, 3$; Fig. 10 shows trajectories of virtual control and actual control $v(t)$

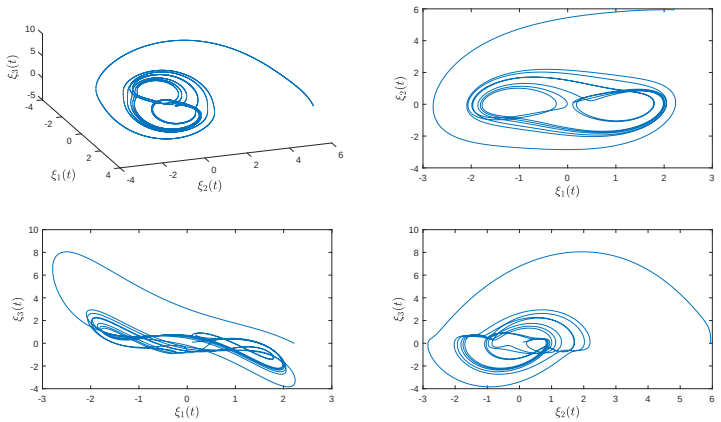


**Fig. 8** The chaotic behaviour of the fractional-order Arneodo system.

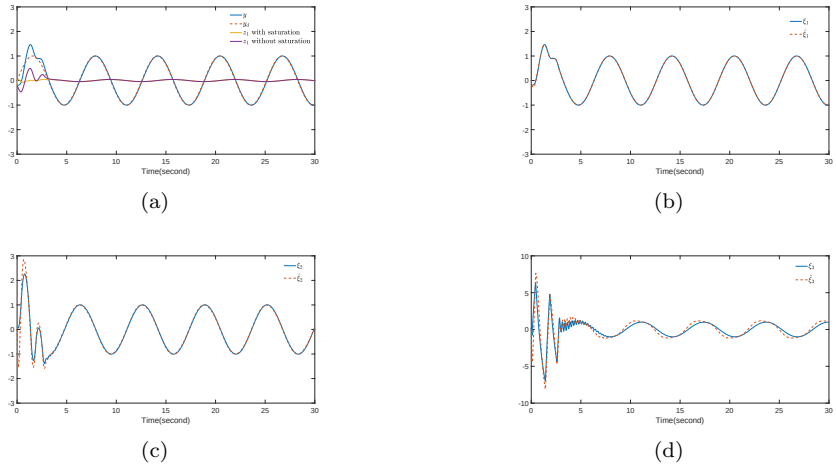


**Fig. 9** Simulation results . (a) Trajectories of the output $y$ and the reference signal $y_d$. (b) Trajectories of $\xi_1$ and estimation $\hat{\xi}_1$. (c) Trajectories of $\xi_2$ and estimation $\hat{\xi}_2$. (d) Trajectories of $\xi_3$ and estimation $\hat{\xi}_3$.

as well as $u(v)$, and the convergence performance of neural network weight parameters is also shown.

## 5 Conclusion

In this paper, an adaptive neural backstepping tracking control scheme is proposed for uncertainty FONSs subject to input saturation and unknown external disturbance. Two observers are constructed to cope with the unavail-

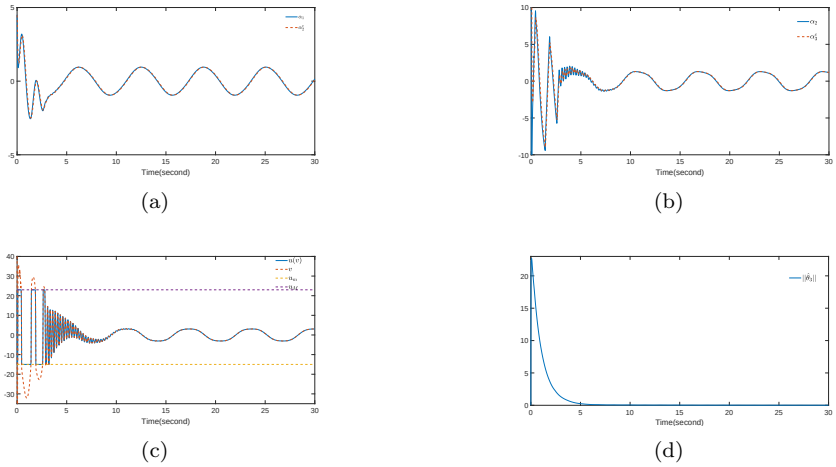


(a) (b)

(c) (d)

**Fig. 10** (a) Trajectories of $\alpha_1$ and $\alpha_2^c$. (b) Trajectories of $\alpha_2$ and $\alpha_3^c$. (c) Control input $u(v)$ and $v$. (d) Trajectory of the neural network parameters $||\hat{\boldsymbol{\theta}}_3||$.

able state and the unknown compound disturbance, and then a robust tracking controller is designed based on fractional Lyapunov stability theory. Under the proposed control scheme, the tracking errors and the state estimation errors have been quickly converged to a small region of the origin. On the other hand, output constraints and unknown control direction which will limit the application of the mentioned method, are often encountered in industry. Therefore, how to design an adaptive neural output feedback control for FONSs with the above restrictions is one of future research directions.

**Acknowledgements** The work is supported by the National Natural Science Foundation of China under Grant No. 11771263.

## Data Availability Statement

Data sharing is not applicable to this article since no associated data.

## Declarations

**Conflict of interest** The authors declare that they have no conflict of interest.

## References

1. H. Sun, Y. Zhang, D. Baleanu, W. Chen, and Y. Chen, "A new collection of real world applications of fractional calculus in science and engineering," *Communications in Nonlinear Science and Numerical Simulation*, vol. 64, pp. 213–231, 2018.

2. K. Rabiei, Y. Ordokhani, and E. Babolian, "Fractional-order boubaker functions and their applications in solving delay fractional optimal control problems," *Journal of Vibration and Control*, vol. 24, no. 15, pp. 3370–3383, 2018.
3. C. Jorge M, R. Juan, C. C Rodrigo, G. Arturo, and A. Juan Gabriel, "A closed form expression for the gaussian–based caputo–fabrizio fractional derivative for signal processing applications," *Communications in Nonlinear Science and Numerical Simulation*, vol. 61, pp. 138–148, 2018.
4. L. Wang, Y. Tang, Y. Chai, and F. Wu, "Generalized projective synchronization of the fractional-order chaotic system using adaptive fuzzy sliding mode control," *Chinese Physics B*, vol. 23, no. 10, p. 100501, 2014.
5. H. Liu, H. Wang, J. Cao, A. Alsaedi, and T. Hayat, "Composite learning adaptive sliding mode control of fractional-order nonlinear systems with actuator faults," *Journal of the Franklin Institute*, vol. 356, no. 16, pp. 9580–9599, 2019.
6. C. Hua, J. Ning, G. Zhao, and Y. Li, "Output feedback nn tracking control for fractional-order nonlinear systems with time-delay and input quantization," *Neurocomputing*, vol. 290, pp. 229–237, 2018.
7. A. Boulkroune, M. Msaad, and M. Farza, "Adaptive fuzzy system-based variable-structure controller for multivariable nonaffine nonlinear uncertain systems subject to actuator nonlinearities," *Neural Computing and Applications*, vol. 28, no. 11, pp. 3371–3384, 2017.
8. H. Liu, S. Li, H. Wang, and Y. Sun, "Adaptive fuzzy control for a class of unknown fractional-order neural networks subject to input nonlinearities and dead-zones," *Information Sciences*, vol. 454, pp. 30–45, 2018.
9. C. W. Anderson, "Learning to control an inverted pendulum using neural networks," *IEEE Control Systems Magazine*, vol. 9, no. 3, pp. 31–37, 1989.
10. T. Chen, D. Cao, J. Yuan, and H. Yang, "Observer-based adaptive neural network backstepping sliding mode control for switched fractional order uncertain nonlinear systems with unmeasured states," *Measurement and Control*, p. 00202940211021107, 2021.
11. J. Ni, L. Liu, C. Liu, and X. Hu, "Fractional order fixed-time nonsingular terminal sliding mode synchronization and control of fractional order chaotic systems," *Nonlinear dynamics*, vol. 89, no. 3, pp. 2065–2083, 2017.
12. Y. Li, Y. Liu, and S. Tong, "Observer-based neuro-adaptive optimized control of strict-feedback nonlinear systems with state constraints," *IEEE Transactions on Neural Networks and Learning Systems*, 2021.
13. M. K. Shukla and B. Sharma, "Stabilization of a class of fractional order chaotic systems via backstepping approach," *Chaos, Solitons & Fractals*, vol. 98, pp. 56–62, 2017.
14. S. Han, "Fractional-order command filtered backstepping sliding mode control with fractional-order nonlinear disturbance observer for nonlinear systems," *Journal of the Franklin Institute*, vol. 357, no. 11, pp. 6760–6776, 2020.
15. C. Wang, L. Cui, M. Liang, J. Li, and Y. Wang, "Adaptive neural network control for a class of fractional-order nonstrict-feedback nonlinear systems with full-state constraints and input saturation," *IEEE Transactions on Neural Networks and Learning Systems*, 2021.
16. H. Liu, Y. Pan, S. Li, and Y. Chen, "Adaptive fuzzy backstepping control of fractional-order nonlinear systems," *IEEE Transactions on Systems, Man, and Cybernetics: Systems*, vol. 47, no. 8, pp. 2209–2217, 2017.
17. S. B. Fazeli Asl and S. S. Moosapour, "Fractional order fuzzy dynamic backstepping sliding mode controller design for triaxial mems gyroscope based on high-gain and disturbance observers," *IETE Journal of Research*, pp. 1–18, 2019.
18. H. Liu, Y. Pan, and J. Cao, "Composite learning adaptive dynamic surface control of fractional-order nonlinear systems," *IEEE Transactions on Cybernetics*, vol. 50, no. 6, pp. 2557–2567, 2019.
19. Z. Ma and H. Ma, "Adaptive fuzzy backstepping dynamic surface control of strict-feedback fractional-order uncertain nonlinear systems," *IEEE Transactions on Fuzzy Systems*, vol. 28, no. 1, pp. 122–133, 2019.
20. A. Mujumdar, B. Tamhane, and S. Kurode, "Observer-based sliding mode control for a class of noncommensurate fractional-order systems," *IEEE/ASME Transactions on Mechatronics*, vol. 20, no. 5, pp. 2504–2512, 2015.

21. D. Sheng, Y. Wei, S. Cheng, and Y. Wang, "Observer-based adaptive backstepping control for fractional order systems with input saturation," *ISA transactions*, vol. 82, pp. 18–29, 2018.
22. S. Lu and X. Wang, "Observer-based command filtered adaptive neural network tracking control for fractional-order chaotic pmsm," *IEEE access*, vol. 7, pp. 88777–88788, 2019.
23. S. Luo, S. Li, F. Tajaddodianfar, and J. Hu, "Observer-based adaptive stabilization of the fractional-order chaotic mems resonator," *Nonlinear Dynamics*, vol. 92, no. 3, pp. 1079–1089, 2018.
24. J. Ma, Z. Zheng, and P. Li, "Adaptive dynamic surface control of a class of nonlinear systems with unknown direction control gains and input saturation," *IEEE transactions on cybernetics*, vol. 45, no. 4, pp. 728–741, 2014.
25. S. Song, B. Zhang, X. Song, and Z. Zhang, "Neuro-fuzzy-based adaptive dynamic surface control for fractional-order nonlinear strict-feedback systems with input constraint," *IEEE Transactions on Systems, Man, and Cybernetics: Systems*, 2019.
26. M. Chen, S. Shao, and B. Jiang, "Adaptive neural control of uncertain nonlinear systems using disturbance observer," *IEEE Transactions on Cybernetics*, vol. 47, no. 10, pp. 3110–3123, 2017.
27. Z. S. Aghayan, A. Alfi, and J. Tenreiro Machado, "Stability analysis of fractional order neutral-type systems considering time varying delays, nonlinear perturbations, and input saturation," *Mathematical Methods in the Applied Sciences*, vol. 43, no. 17, pp. 10332–10345, 2020.
28. A. Razzaghian, R. Kardehi Moghaddam, and N. Pariz, "Fractional-order nonsingular terminal sliding mode control via a disturbance observer for a class of nonlinear systems with mismatched disturbances," *Journal of Vibration and Control*, vol. 27, no. 1-2, pp. 140–151, 2021.
29. S. Li, Z. Xiang, H. Lin, and H. R. Karimi, "State estimation on positive markovian jump systems with time-varying delay and uncertain transition probabilities," *Information Sciences*, vol. 369, pp. 251–266, 2016.
30. I. Podlubny, *Fractional differential equations: an introduction to fractional derivatives, fractional differential equations, to methods of their solution and some of their applications*. Elsevier, 1998.
31. H. Liu, S. Li, H. Wang, and G. Li, "Adaptive fuzzy synchronization for a class of fractional-order neural networks," *Chinese Physics B*, vol. 26, no. 3, p. 030504, 2017.
32. P. Gong and W. Lan, "Adaptive robust tracking control for uncertain nonlinear fractional-order multi-agent systems with directed topologies," *Automatica*, vol. 92, pp. 92–99, 2018.
33. B. Chen, H. Zhang, and C. Lin, "Observer-based adaptive neural network control for nonlinear systems in nonstrict-feedback form," *IEEE transactions on neural networks and learning systems*, vol. 27, no. 1, pp. 89–98, 2015.
34. S. Luo, F. L. Lewis, Y. Song, and K. G. Vamvoudakis, "Adaptive backstepping optimal control of a fractional-order chaotic magnetic-field electromechanical transducer," *Nonlinear Dynamics*, pp. 1–18, 2020.
35. S. Sui, C. P. Chen, and S. Tong, "Neural-network-based adaptive dsc design for switched fractional-order nonlinear systems," *IEEE Transactions on Neural Networks and Learning Systems*, 2020.
36. M. A. Balootaki, H. Rahmani, H. Moeinkhah, and A. Mohammadzadeh, "On the synchronization and stabilization of fractional-order chaotic systems: Recent advances and future perspectives," *Physica A: Statistical Mechanics and its Applications*, vol. 551, p. 124203, 2020.